

Preparation of Syndiotactic Polystyrene/Montmorillonite Nanocomposites via *In Situ* Intercalative Polymerization of Styrene with Monotitanocene Catalyst

Zhigang Shen,^{1,2} Fangming Zhu,¹ Dan Liu,¹ Xiguo Zeng,¹ Shangan Lin¹

¹Institute of Polymer Science, School of Chemistry and Chemical Engineering, Zhongshan University, Guangzhou 510275, China

²Shanghai Research Institute of Petrochemical Technology, China Petrochemical Corporation, Shanghai 201208, China

Received 1 May 2004; accepted 28 August 2004

DOI 10.1002/app.21369

Published online in Wiley InterScience (www.interscience.wiley.com).

ABSTRACT: Syndiotactic polystyrene (sPS)/montmorillonite nanocomposites were prepared via *in situ* intercalative coordination polymerization using mono-(η^5 -pentamethylcyclopenta-dienyl) tribenzoyloxy titanium [$\text{Cp}^*\text{Ti}(\text{OBz})_3$] complex activated by methylaluminumoxanes (MAO) and triisobutylaluminum (TIBA). The influences of polymerization conditions, such as the weight ratio of montmorillonite and styrene, temperature, and monomer concentration, on the preparation of sPS/montmorillonite nanocomposites was investigated. The intercalation spacing in the nanocomposites, as well as the exfoliation of the montmorillonite interlayers, was characterized with wide angle X-ray diffraction (WAXD) and transmission electron microscopy (TEM). The dispersibility of the

nanoscale elements depended on the polymerization conditions and the surfactant treatment. The crystallizability and thermal properties of these nanocomposites were determined by differential scanning calorimetry (DSC) analysis and thermogravimetric analysis (TGA). Experimental results indicated that the degree of crystallinity of the sPS nanocomposite increased with increasing montmorillonite content and with higher T_g and thermal decomposition temperature than pure sPS. © 2005 Wiley Periodicals, Inc. *J Appl Polym Sci* 95: 1412–1417, 2005

Key words: metallocene catalysts; syndiotactic polystyrene; nanocomposites

INTRODUCTION

Syndiotactic polystyrene (sPS) has attracted considerable interest for its properties and many potential applications.^{1–6} In contrast to the well-known isotactic polystyrene (iPS), the sPS displays a fast crystallization rate, more than an order of magnitude higher than that of iPS, and a high crystallinity.⁷ These, along with its high melting point (270°C), superior heat and chemical resistance, high modulus of elasticity, enhanced mechanical properties, and low water absorbability, give sPS potential as an engineering thermoplastic. However, its inherent brittleness and poor impact and tear resistance limit it for some end uses.

Nanocomposites are defined by the particle size of the dispersed phase having at least one dimension less than 100 nm. Because of the nanoscale feature, nanocomposites possess superior physical and mechanical behavior over their more conventional microcomposites counterparts. Thermoplastic polymers/montmorillonite (clay) nanocomposites have also received much interest owing to their ability to provide substantial property enhancement by their large aspect

ratio and surface area of the dispersed montmorillonite.^{8–12} The montmorillonite consists of ordered nanometer-thick silicate plates that form a hydrophilic layer structure, which hinders the intercalation of organic polymers or monomers. Modified by surfactant (intercalative reagent), the reduction in surface energy improves the organophilic characteristics of the montmorillonite surface, so it is possible that polymers or monomers intercalate into montmorillonite. The intercalation causes the interlayer spacing to expand and/or interlayer exfoliation to occur, producing polymer matrix nanocomposites. Melt or solution intercalation of polymers and *in situ* polymerization in the montmorillonite interlayers are the two most common ways to prepare polymers/montmorillonite nanocomposites.^{13–15} In recent years, sPS/montmorillonite nanocomposites have been developed and have attracted great interest from industries and academic.^{16–18} However, it is difficult to prepare these nanocomposites by melt and solution blending because sPS possesses a high melting temperature and solvent resistance. The disadvantage of preparing sPS/montmorillonite nanocomposites by melt blending is that the microstructure of montmorillonite will be destroyed, as well as the intercalative reagent separating from its interlayer, since the melting temperature required for sPS is higher than 270°C.¹⁹ The sPS/

Correspondence to: F. Zhu (ceszfm@zsu.edu.cn).

montmorillonite nanocomposites have been prepared by mixing the montmorillonite with dissolved sPS in dichlorobenzene at 140°C.²⁰ The dispersibility of the nanoscale element significantly affects the chain conformation and crystallization of sPS. However, much solvent must be used.

Monotitanocene/methylaluminoxane (MAO) catalysts have been found to be most favorable for syndiospecific polymerization of styrene.^{21–30} One promising strategy for preparing sPS/montmorillonite nanocomposites is by the intercalation of the organometallic catalyst and monomer into the layered montmorillonite and then polymerization *in situ*. For this paper a new monotitanocene/MAO catalyst was designed and synthesized. Syndiotactic polystyrene/montmorillonite nanocomposites were prepared *in situ* via intercalative coordination polymerization with this catalyst. The interlayer spacing in the nanocomposites and the degree of dispersion of these composites was investigated with various modern characterization techniques.

EXPERIMENTAL

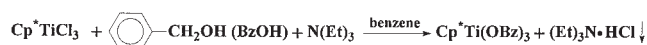
Materials

Toluene was refluxed over metallic sodium for 24 h and distilled under nitrogen atmosphere before use. Styrene was purified by stirring over CaH₂ for about 24 h and then distilled under reduced pressure over CaH₂ and was finally stored under nitrogen atmosphere. Trimethylaluminum (TMA) and triisobutylaluminum (TIBA) from Ethyl Company were used as received.

The montmorillonite (MT) was purchased from the Third Reagent Factory of Shanghai. It has an ion-exchange capacity of 96.0 mEq/100 g. The surface of the natural sodium montmorillonite was modified by cationic exchange in an aqueous solution with an intercalative reagent of hexadecyl trimethylammonium chloride at 60°C for 4 h. The dispersed solution was filtered and repeatedly washed with deionized water to remove excess intercalative reagent, that is, until there was no white precipitate observed in the wash water when tested by a 0.1 mol/L AgNO₃ solution. The product was then vacuum dried to a constant weight and ground into powder (diameter about 40–60 μm) to get the modified montmorillonite (MMT).

η^5 -Pentamethylcyclopentadienyltribenzyloxy titanium [Cp*Ti(OBz)₃] was prepared by the reaction of η^5 -pentamethylcyclopentadienyltrichloride titanium (Cp*TiCl₃) with benzyl alcohol in the presence of an absorbent for HCl [such as N(Et)₃] as shown in the Scheme 1.

A yellow liquid product (yield 89%) was obtained. Anal. Calcd for C₃₁H₃₆O₃Ti: C:73.81, H: 7.14; Found:



Scheme 1

C:73.26, H: 7.02. Methylaluminoxane (MAO) was prepared by first controlled reaction of trimethylaluminum (TMA) with H₂O from Al₂(SO₄)₃ · 18H₂O dispersed in toluene for several hours, then filtration, and finally evaporation under vacuum.

Intercalative polymerization of styrene

The polymerization runs were carried out under an extra-pure-grade nitrogen atmosphere in 250-mL glass flasks equipped with a magnetic stirrer. The MMT or MT, MAO, 1M TIBA hexane solution, toluene, and Cp*Ti(OBz)₃ were added. The solution was stirred at 70°C for 20 min and then styrene was introduced into the reactor. The polymerizations were terminated by the addition of 10 wt % HCl in ethanol. The syndiotactic polystyrene/montmorillonite nanocomposites were washed with ethanol and dried in vacuum at 80°C to constant weight. The pure sPS was also synthesized by Cp*Ti(OBz)₃/MAO/TIBA catalyst without fixing on the montmorillonite in the same polymerization conditions, as a reference for the sPS/montmorillonite nanocomposites.

Characterization

The viscosity-average molecular weights (M_v) of the polymers were calculated from $[\eta]$ measured in *o*-dichlorobenzene at 135°C for sPS. ¹³C-NMR spectra of sPS were recorded at 120°C in *o*-dichlorobenzene using an INOVA 500 MHz spectrometer and referenced versus TMS as standard. The sPS samples were dissolved in *o*-dichlorobenzene/benzene-*d*₆ to form a 15 wt % solution. A D/MAX-3AX diffractometer was used to obtain patterns by using a Ni-filtered Cu-K_α X-ray beam, and Bragg's law ($\lambda = 2d \sin \theta$, $\lambda = 0.154$ nm) was used to compute the spacing. The nanometer structure of the nanocomposites was investigated by a Hitachi (Japan) H-600 transmission electron microscope (TEM) with an acceleration voltage of 100 kV. The ultrathin slides were obtained by sectioning the injection-molded samples with a diamond knife. Differential scanning calorimetry (DSC) analysis was conducted with a Perkin-Elmer DCS-7 system. Data reported were gathered, for the second melting with a heating and cooling scan of 10°C/min. Thermogravimetric analysis (TGA) was carried out with a Shimadzu TGA-50 thermogravimetric analyzer at a heating rate of 20°C/min from 50 to 600°C under a continuous air (50 mL/min) purge.

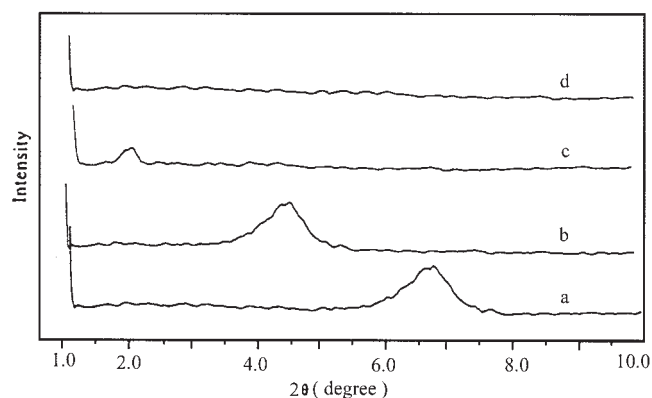


Figure 1 WAXD patterns of (a) MT, (b) MMT and sPS/MMT nanocomposites obtained from (c) Run 5 and (d) Run 4 in Table I.

RESULTS AND DISCUSSION

In situ intercalative polymerization of styrene with $\text{Cp}^*\text{Ti}(\text{OBz})_3/\text{MAO}/\text{TIBA}$ catalyst

The size of organo-montmorillonite or MMT interlayers was about 2 nm, determined by WAXD, as shown in Figure 1(b). Therefore the organic compounds, including MAO, TIBA, and $\text{Cp}^*\text{Ti}(\text{OBz})_3$, were easily able to enter the interlayers and form, *in situ*, the active species for styrene syndiospecific polymerization. According to the intercalative coordination polymerization mechanism, *in situ* polymerization was performed in the MMT interlayers as soon as the styrene molecules intercalated in the interlayers. The polymerization conditions, catalytic activity, montmorillonite content in yields, syndiotacticity of polystyrene, and glass transition temperature (T_g), as well as melting temperature (T_m), of sPS are shown in Table I. It should be noted that syndiospecific polymerization of styrene displayed high activity, with $\text{Cp}^*\text{Ti}(\text{OBz})_3/$

MAO/TIBA homogeneous catalyst, and the addition of MMT did not influence the polymerization behavior. The resultant polymers were analyzed by ^{13}C -NMR and DSC and shown to be highly syndiotactic polystyrene with a T_g of $98.6 \approx 112.7^\circ\text{C}$ and T_m of $269.8 \approx 270.6^\circ\text{C}$. It is interesting that, with increasing MMT content, the T_g of sPS is noticeably increased. In contrast, when the styrene was polymerized with $\text{Cp}^*\text{Ti}(\text{OBz})_3/\text{MAO}/\text{TIBA}$ in the presence of montmorillonite without modification by organo intercalative reagent, there was extremely low polymerization activity. The reason is that the hydrophilic surface of the montmorillonite is poisonous to the catalyst.

Microstructure of sPS/montmorillonite nanocomposites

Figure 1 shows the WAXD patterns of MT, MMT, and sPS/MMT nanocomposites. The MT and MMT display their characteristic peaks at $2\theta = 6.7$ and 4.5° , respectively, corresponding to the (001) diffraction of layer structure of the MT and MMT, indicating that the interlayer spacing between silicate layers was expanded from 1.3 to 2.0 nm by an intercalative reagent of hexadecyl trimethylammonium chloride. However, the characteristic peak disappears at $2\theta = 1.7^\circ$ in the WAXD pattern of sPS/MMT nanocomposites containing 6.0 wt % MMT, as shown in Figure 1(c), suggesting that the interlayer spacing of the MMT in the nanocomposite is not less than 5.2 nm. As shown in Figure 1(d), no characteristic peak was found in the WAXD pattern of sPS/MMT nanocomposite with the MMT of 4.5 wt %, which implied that the nanocomposite was possibly exfoliated. These results indicate that the styrene molecules intercalated into the MMT interlayer and polymerized *in situ* and that the layer structure of the MMT was expanded and even destroyed by sPS molecular chains.

TABLE I
Preparation of Syndiotactic Polystyrene/Montmorillonite (MT) Nanocomposites with $\text{Cp}^*\text{Ti}(\text{OBz})_3/\text{MAO}/\text{TIBA}$ Catalyst^a

Run no.	MT/St. (g/g)	Yield (wt %)	Activity $\times 10^{-6}$ (gPS/molTi \cdot h)	sPS ^a (wt %)	MT wt % in yield	T_g^b ($^\circ\text{C}$)	T_m^b ($^\circ\text{C}$)	ΔH_m^b (J/g)
1	0	70.3	2.9	97.2	0	98.6	269.8	23.58
2	1 : 99	68.2	2.8	98.0	1.5	101.3	270.1	24.69
3	2 : 98	69.8	2.9	97.5	2.9	105.1	268.5	26.78
4	3 : 97	66.9	2.7	96.6	4.5	106.4	269.2	27.32
5	4 : 96	70.1	2.9	97.4	6.0	109.8	270.6	27.56
6	5 : 95	69.6	2.9	96.7	7.5	112.7	270.0	27.38
7 ^c	3 : 97	trace	trace	/	≈ 100	/	/	/

Polymerization Conditions: $[\text{Ti}] = 1.4 \times 10^{-4}$ mol/L, $[\text{St.}] = 5.8$ mol/L, $\text{Al}_{\text{MAO}}/\text{Ti} = 400$ (mol/mol), $\text{Al}_{\text{TIBA}}/\text{Ti} = 200$ (mol/mol), toluene used as solvent, polymerization temperature = 80°C , polymerization time = 1 h.

^a Syndiotacticity of polystyrene determined by ^{13}C -NMR.

^b Glass transition temperature, melting temperature, and melting enthalpy determined by DSC.

^c Montmorillonite used without being modified by surfactant.

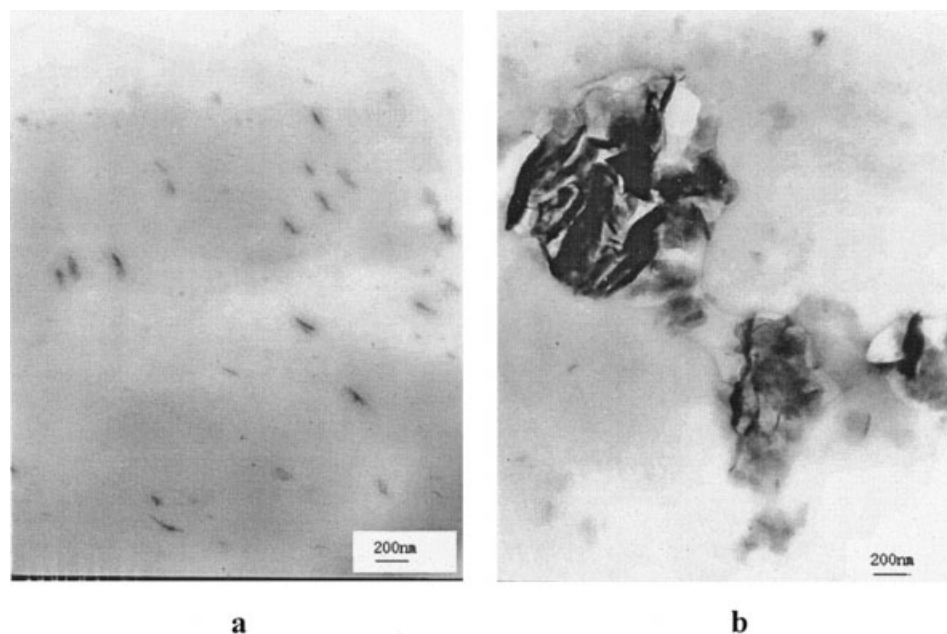


Figure 2 TMA micrographs of (a) 4.5 wt % sPS/MMT nanocomposite obtained from Run 4 in Table I and (b) 4.5 wt % sPS/MMT composite prepared by melt blending.

TEM micrographs can provide further evidence for montmorillonite dispersibility in sPS matrix prepared via *in situ* intercalative polymerization with $\text{Cp}^*\text{Ti}(\text{OBz})_3/\text{MAO}/\text{TIBA}$ catalyst. Figure 2(a) presents a TEM micrograph of a sPS/MMT nanocomposite with the MMT of 4.5 wt % obtained from Run 4 in Table I, where the small dark points denote the aggregation of silicate layers. The dark points were dispersed homogeneously in the sPS matrix and the size was less than 40 nm, from which it is supposed that the montmorillonite was partially exfoliated. Figure 2(b) shows the TEM micrograph of sPS/MMT composite with 4.5 wt % MMT prepared by melt blending for 10 min at 290°C, where the dark regions denote the MMT particles: the size of these is about 40–60 μm , the same as the size of the added MMT powders, indicating that the layers of montmorillonite were unexfoliated. Actually, about 70 wt % of the alkyl ammonium material was degraded at 280°C²⁰ and, at the same time, as shown in Figure 3, the interlayer spacing decreases from 2.0 to 1.3 nm, which is that of MT due to desorption of the intercalative reagent (hexadecyl trimethylammonium). Therefore, the sPS molecular chains cannot enter in to the montmorillonite interlayers.

Thermal characterization of sPS/montmorillonite nanocomposites

The results of DSC analysis of sPS/MMT nanocomposites are shown in Table I. The glass transition temperature (T_g) of nanocomposites had an evident in-

crease from 98.6 to 112.7°C corresponding to 0 \approx 7.5 wt % MMT. This demonstrates that the better dispersibility of the montmorillonite in the sPS matrix increases the interaction between sPS molecular chains and montmorillonite nanoparticles, which hinders the sPS segment motion. The melting temperatures (T_m) of pure sPS and sPS/MMT nanocomposites were all about 270°C. However, the enthalpy of melting (ΔH_m) of sPS/MMT nanocomposites is higher than pure sPS, indicating that sPS/MMT nanocomposites possess higher degrees of crystallinity. Figure 4 shows the cooling curves of pure sPS and sPS/MMT nanocomposites from 278°C to room temperature at a cooling

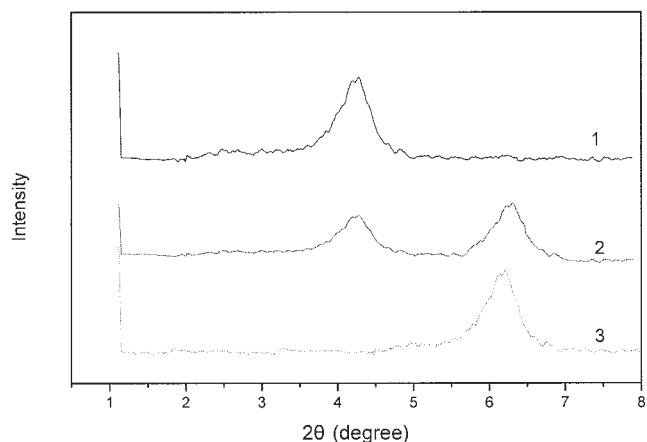


Figure 3 WAXD patterns of MMT (1) and sPS/MMT composites prepared by melt blending for 5 min (2) and 10 min (3) at 290°C.

rate of 10°C/min. The crystallization temperature was increased and the crystallization peaks gradually became narrow as the content of montmorillonite in sPS matrix increased, implying that the sPS crystallization rate increased. The montmorillonite nanoparticles can act as an efficient nucleating agent to facilitate sPS crystallization.

The thermal stabilities of the sPS/MMT nanocomposites and pure sPS, studied by TGA analysis, are shown in Figure 5. In a comparison of the thermal decomposition temperature of the sPS/MMT nanocomposites with that of the pure sPS, the thermal stability of the nanocomposites is much higher than that of pure sPS. The onset of the thermal decomposition temperature of the nanocomposite was shifted to higher temperatures with increasing montmorillonite content. It shows that, by introducing about 6.0 wt % montmorillonite in the nanocomposite, the thermal decomposition temperature increased 50°C over that of the pure sPS.

CONCLUSION

sPS/montmorillonite nanocomposites were successfully prepared via *in situ* intercalative polymerization with $\text{Cp}^*\text{Ti}(\text{OBz})_3/\text{MAO}/\text{TIBA}$ catalyst, when the montmorillonite was modified by hexadecyl trimethylammonium chloride used as an intercalative reagent. The WAXD patterns and TEM image showed that the montmorillonite in the nanocomposites was partially exfoliated into nanometer size (less than 40 nm) and dispersed uniformly in the sPS matrix. The degree of crystallinity of the sPS/montmorillonite nanocomposite is higher than pure sPS. The montmorillonite functions as a nucleating agent to increase the crystal-

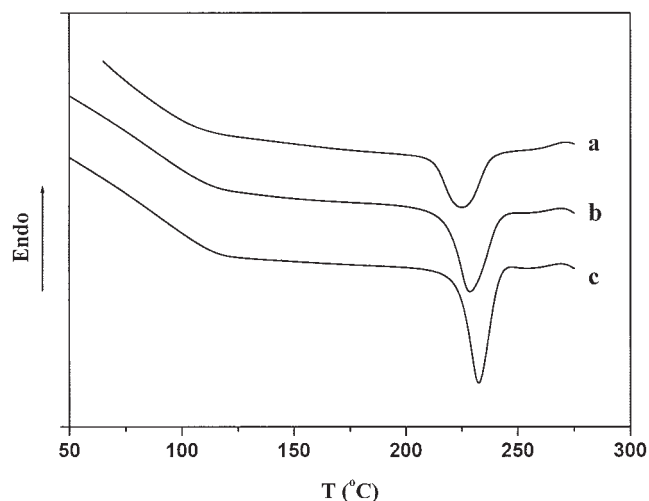


Figure 4 DSC cooling curves of sPS and sPS/MMT nanocomposites obtained from (a) Run 1, (b) Run 4, and (c) Run 5 in Table I.

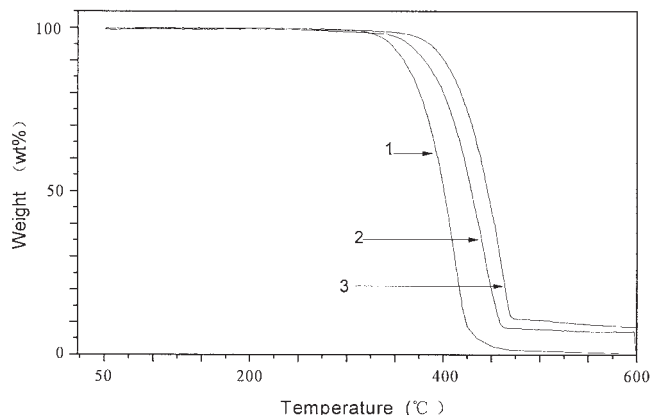


Figure 5 Thermogravimetric analysis of sPS and sPS/MMT nanocomposites obtained from (1) Run 1, (2) Run 4, and (3) Run 5 in Table I.

lization rate of the sPS matrix. The T_g of the nanocomposites increases significantly with increasing montmorillonite content, and the T_m does slightly, too. The thermal resistance of the nanocomposites is significantly increased. The temperature of the derivative weight loss of sPS/MMT (6.0 wt %) was higher than that of pure sPS by 50°C.

The financial support of the Guangdong Provincial Natural Science Foundation of China (contract grant number 039184) is gratefully acknowledged.

References

- Woo, E. M.; Wu, F. S. *J Polym Sci, Part B: Polym Phys* 1998, 36, 2725.
- Moyses, S.; Spells, S. J. *Polymer* 1998, 39, 3665.
- Rose, C. D.; Rizzo, P.; Ballesteros, O. R.; Petraccone, V.; Guerra, G. *Polymer* 1999, 40, 2103.
- Tsutsui, K.; Katsumata, T.; Yamamoto, Y.; Fukatsu, H.; Yoshimizu, H.; Kinoshita, T.; Tsujita, Y.; *Polymer* 1999, 40, 3815.
- Malanga, M. *Adv Mater* 2000, 12, 1869.
- Ray, B.; Elhasri, S. Thierry, A.; Marie, P.; Guenet, J. M. *Macromolecules* 2002, 35, 9730.
- Giantotti, G.; Valvassori, A. *Polymer* 1990, 31, 473.
- Ginzburg, V. V.; Singh, C.; Balazs, A. C. *Macromolecules* 2000, 33, 1089.
- Koo, C. M.; Kim S. O.; Chung, I. J. *Macromolecules* 2003, 36, 2748.
- Mayer, S.; Zentel, R.; Wilhelm, M.; Greiner, A. *Macromol Chem Phys* 2002, 203, 1743.
- Koo, C. M.; Ham, H. T.; Kim S. O.; Wang, K. H.; Chung, I. J.; Kim, D. C.; Zin, W. C. *Macromolecules* 2002, 35, 5116.
- Zeng, C. C.; Lee, L. J. *Macromolecules* 2001, 34, 4098.
- Ishida, H.; Campbell, S.; Blackwell, J. *Chem Mater* 2000, 12, 1260.
- Ray, S. S.; Okamoto, M. *Prog Polym Sci* 2003, 28, 1539.
- Ma, J.; Xu, H.; Ren, J. H.; Yu, Z. Z.; Mai, Y. W. *Polymer* 2003, 44, 4619.
- Wu, H. D.; Tseng, C. R.; Chang, F. C. *Macromolecules* 2001, 34, 2992.
- Wang, Z. M.; Chung, T. C.; Gilman, J. W.; Manias, E. *J Polym Sci Part B: Polym Phys* 2003, 41, 3173.

18. Wu, T. M.; Hsu, S. F.; Wu, J. Y. *J Polym Sci Part B: Polym Phys* 2003, 41, 1730.
19. Il Park, C.; Park, O. O.; Lim, J. G.; Kim, H. J. *Polymer* 2001, 42, 7465.
20. Tseng, C. R.; Wu, J. Y.; Lee, H. Y.; Chang, F. C. *Polymer* 2001, 42, 10063.
21. Ishihara, N.; Seimiya, T.; Kuramoto, M.; Uoi, M. *Macromolecules* 1986, 19, 2464.
22. Zambelli, A.; Oliva, L.; Pellicchia, C. *Macromolecules* 1989, 22, 2129.
23. Po, R.; Cardi, N. *Prog Polym Sci* 1996, 21, 47.
24. Grassi, A.; Zambelli, A. *Organometallics* 1996, 15, 480.
25. Wu, Q.; Ye, Z.; Lin, S. A. *Macromol Chem Phys* 1997, 198, 1823.
26. Zhu, F. M.; Lin, S. *Chem J Chin Univ* 1997, 18, 2065.
27. Flores, J. C.; Ready, T. E.; Chien, J. C. W.; Rausch, M. D. *J Organomet Chem* 1998, 562, 11.
28. Schwecke, C.; Kaminsky, W. J. *Polym Sci, Part A: Polym Chem* 2001, 39, 2805.
29. Schellenberg, J.; Tomotsu, N. *Prog Polym Sci* 2002, 27, 1925.
30. Nifant'ev, I. E.; Yu, L.; Besedin, D. V. *Organometallics* 2003, 22, 2619.